AIAA JOURNAL
Vol. 33, No. 8, August 1995

Dynamic Recovery to Fully Attached Aerofoil Flow from Deep Stall

R. B. Green* and R. A. McD. Galbraith†
University of Glasgow, Glasgow G12 8QQ, Scotland, United Kingdom

This paper presents results from a comprehensive analysis of pressure data from several two-dimensional aerofoil models performing constant pitch rate "ramp-down" motions from the fully separated state to the fully attached state. The salient observation is that, a short while after reattachment is first observed at the leading edge, a weak disturbance travels from the leading edge to the trailing edge, and this disturbance causes a characteristic wave on the pressure data. The speed of the wave is uniform along the chord and is predominantly independent of aerofoil profile and reduced pitch rate. This contrasts with the rate of attachment, which is strongly pitch rate dependent. It is suggested that the wave indicates convection of wake fluid over the aerofoil surface.

Nomenclature

C_N	= normal force coefficient
$C_{N\min}$	= local minimum value of C_N
C_p	= pressure coefficient
$C_{p\,\mathrm{dev}}$	= characteristic change of rate of decrease of suction
c	= model chord length, m
f	= attachment position, measured from the leading edge (expressed as fraction of chord length)
Re	= Reynolds number based on chord length
r	= reduced pitch rate, $\omega c/2U$
t	= time, s
U	= freestream velocity, ms^{-1}
u_r	= rate of attachment along the chord, ms^{-1}
u_w	= ramp-down wave speed along aerofoil chord, ms^{-1}
x	= chordwise position from leading edge, m
α	= incidence, deg
Δt	= ramp-down time delay, s
τ	= nondimensional ramp-down time delay, $\Delta tU/c$
τ_m	= average nondimensional ramp-down time delay
ω	= pitch rate, $(2\pi\,\mathrm{d}\alpha/\mathrm{d}t)/360$, rad s^{-1}

I. Introduction

CORRECT helicopter rotor design must account for the effects of unsteady aerodynamics; as a helicopter blade rotates around the azimuth, the effective dynamic pressure changes, and the blade is pitched up or down to compensate for this. The overwhelming interest in two-dimensional aerofoil unsteady aerodynamics has been dynamic stall. It is well known that as an aerofoil pitches up, stall is delayed to significantly higher angles of incidence, and that stall itself is a violent event, characterized by the formation of a powerful vortex. For details of the dynamic stall process and convection of the dynamic stall vortex, the reader is referred to McCroskey et al.,[1] Lorber and Carta,[2] and Green et al.[3] As a consequence of the amount of attention that has been given to dynamic stall, little is known about the aerodynamics of reattachment during unsteady aerofoil motion. An additional complication is that the majority of wind-tunnel testing has been for sinusoidal pitching motions, and the reattachment phenomena cannot therefore be isolated from the dynamic stall transient effects. Constant pitch rate "ramp-down" motions from the fully separated state may alleviate the latter problem, and these tests have been performed as part of a standard test series on 13 aerofoil models at the University of Glasgow (Galbraith et al.[4]).

The important features of the ramp-down aerodynamic data are described as follows. Niven et al.[5] and Niven and Galbraith[6] showed how the normal force varied with incidence as the reduced pitch rate was increased, and Fig. 1, showing ramp-down data for the NACA 0015, is included here for convenience. It can be seen that as incidence decreases from 40 deg, each test follows approximately the same line, and the gradient of each curve remains almost constant until the minimum normal force $C_{N\min}$ occurs. The gradient is only a weak function of the reduced pitch rate and is almost the same as the static value. An important observation from Fig. 1 is that the fully separated, bluff body behavior, normally seen at very high α in the static case, is extended to much lower incidence. Therefore, for convenience the data from high incidence down to the $C_{N\min}$ incidence are termed the "bluff response." Note that at sufficiently high reduced pitch rate, $C_{N\min}$ may be negative, even though the incidence has a large positive value. Niven et al.[5] reported that the incidence of onset of flow attachment at the leading edge was close to the static value, and this is indicated at 18-deg incidence.

Since the phenomenon of negative C_N at large positive incidence was an unusual result, considerable effort was expended in assessing the importance of wind-tunnel constraint. A variety of different test conditions, including the effect of chord size, the addition of fins along the span, and starting the ramp-down test from successively lower incidences, were found to have no significant effect upon the salient features of the data (Niven and Galbraith[6] and Green and Galbraith[7]). It was concluded that effects of three-dimensionality and blockage were secondary, and thus the observations from data such as in Fig. 1 are essentially those from a two-dimensional flow.

Leading-edge attachment and the minimum normal force are two significant features on the ramp-down data. Leading-edge

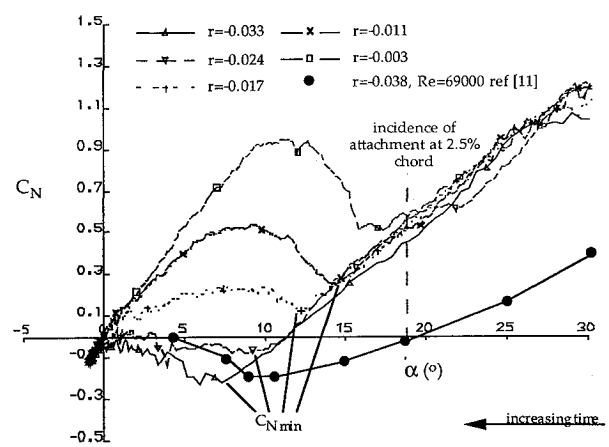

Fig. 1 Plots of C_N vs α during 40- to −1-deg ramp-down tests of the NACA 0015 at $Re = 1.5 \times 10^6$. The effect of reduced pitch rate is shown; $C_{N\min}$ and the incidence of attachment at 2.5% chord are indicated. The bluff response is the behavior down to $C_{N\min}$.

Received Aug. 17, 1994; revision received Feb. 8, 1995; accepted for publication Feb. 13, 1995. Copyright © 1995 by the American Institute of Aeronautics and Astronautics, Inc. All rights reserved.

*Lecturer, Department of Aerospace Engineering.
†Head, Department of Aerospace Engineering.

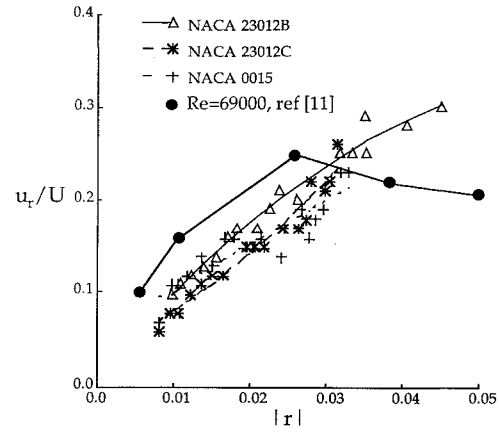

Fig. 2 Rate of attachment for $x/c > 0.1$ as a function of reduced pitch rate for the NACA 23012B, 23012C, and 0015 profiles.

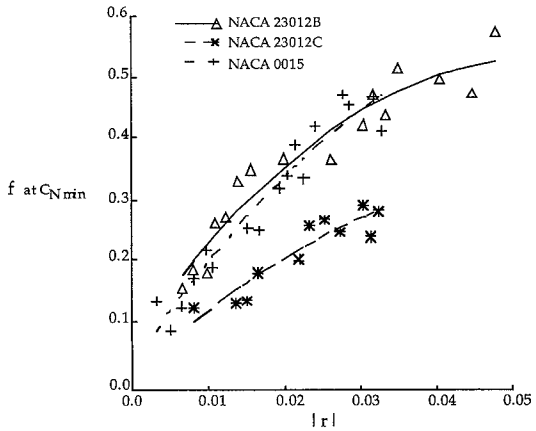

Fig. 3 Variation of chordwise position of attachment f at $C_{N\,min}$ as a function of reduced pitch rate for the NACA 23012B, 23012C, and 0015 aerofoils. As $|r|$ increases, $C_{N\,min}$ occurs when attachment progressively further aft.

attachment represents the start of the return to attached flow behavior, and the minimum normal force indicates the end of the bluff body like behavior. From a comprehensive analysis of the pressure data of Galbraith et al.,[4] Niven et al.[5] and Green and Galbraith[8] assessed the attachment behavior and measured the time delay τ, which is defined as the time elapsed between the first observation of flow reattachment at the leading edge and the occurrence of $C_{N\,min}$. For convenience the important results are described next.

Flow attachment was observed to progress from the leading edge to the trailing edge and is manifested in a particular response on the individual chordwise pressure transducer traces (see Results section). The rate at which attachment progressed along the chord may be inferred from the individual chordwise pressure traces and was observed to be a strong function of reduced pitch rate. Figure 2 shows that the attachment speed u_r increases as $|r|$ increases. This contrasts strongly with the time delay τ, which is independent of the reduced pitch rate; the average value of the time delay in the range $0.01 < |r| < 0.045$ was approximately three chord lengths of travel for a number of aerofoil profiles. As a consequence of the preceding two results, the attachment position at the $C_{N\,min}$ condition is a strong function of r; Fig. 3 shows that as $|r|$ increases, $C_{N\,min}$ occurs when the flow over the aerofoil is progressively more attached.

An additional observation of Green and Galbraith[8] was that a thick sand strip placed at the leading edge significantly slowed down the rate of attachment, although the average value of the time delay was not affected. It was thus concluded that the duration of the ramp-down time delay τ (in the context of the extension of the bluff body behavior to low incidence) was not a function of the delayed attachment during a ramp-down test.

In an attempt to identify other physical phenomena during ramp-down motions, Green and Galbraith[8] also presented results of flow visualization data. These tests were performed at a much lower Reynolds number than the pressure data tests and consequently yielded qualitative data only. However, in addition to the delay in attachment, it was observed that the wake was significantly larger than in a static test, and it was suggested that during dynamic reattachment convection of wake fluid was an additional problem to attachment itself.

An important contribution to the understanding of flow reattachment during oscillatory tests has been made by Ahmed and Chandrasekhara.[9,10] Using a variety of techniques, they observed the delayed attachment reported by Niven et al.[5] and noted the temporary formation of a separation bubble during the reattachment process. Most importantly, they observed that initial leading-edge reattachment occurred close to the static stall angle; this observation was first made by Niven et al.[5] Although some of their results suggest an enlarged wake, they did not comment directly on the effect of the wake fluid on the flowfield. More recently, Schreck et al.[11] performed a series of ramp-down tests on a rectangular finite wing with NACA 0015 cross section. Although the Reynolds number was much lower than the results presented in the present paper (6.9×10^4 compared with 1.5×10^6), similar features were observed. First, the normal force behavior was qualitatively similar to the data described in the present paper, and the basic phenomenon of negative C_N at positive α was observed (note that the effects of three-dimensionality were only slight). Data abstracted from Ref. 11 are shown in Fig. 1, where it can be seen that the general $C_N \sim \alpha$ behavior is the same as the Glasgow data. Second, the rate of attachment was observed to increase as $|r|$ increased, and their data are shown in Fig. 2. The trend at low reduced pitch rate is the same as the Glasgow data, although at higher reduced pitch rate Schreck et al.'s data show a slight reduction in the rate of attachment. Figure 2 indicates that the slope of the NACA 23012B curve might be falling above $|r| = 0.035$, however. In view of the large Reynolds number difference between the two data sets, a direct quantitative comparison is not possible. Another result from Ref. 11 is that the leading-edge attachment initiation incidence at the zero span location falls by 2 deg in the range $-0.05 < r < -0.005$, which is a similar change to that reported by Niven et al.[5] Further reference to the work of Schreck et al.[11] will be made later in this paper.

When considering the extension of the bluff body behavior to lower incidence, the time delay τ is the most important parameter that characterizes the ramp-down data; reattachment itself is a problem of secondary importance. The present paper, therefore, considers the aerodynamic phenomena observed between initial attachment at the leading edge and the end of the bluff response, i.e., $C_{N\,min}$. It will be shown that, shortly after reattachment first commences at the leading edge, a weak disturbance travels along the chord, the speed of which is largely independent of reduced pitch rate and model shape. This contrasts with the attachment behavior, which has been established to be strongly dependent upon the pitch rate. With the aid of flow visualization data, it is suggested that the disturbance reveals convection of wake fluid over the model.

II. Experimental Approach

Pressure Data Tests

The data presented in this paper are primarily from the NACA 23012B and 23012C aerofoil sections tested at the University of Glasgow. These models are based on the NACA 23012; the B derivative is thickened and has a modified lower surface, and the C version has extra camber. Some data from a NACA 0015 are also included in this paper. All of the profiles are shown in Fig. 4. The models tested had a chord length of 0.55 m and a span of 1.61 m. Construction consisted of a fiberglass skin filled with an epoxy foam and bonded to an aluminium spar. The models were mounted vertically in the University of Glasgow's Handley-Page wind tunnel (Fig. 5). This is a closed return type tunnel, with a 1.6×2.13 m octagonal working section. The models were pitched about the quarter-chord point using a linear hydraulic actuator and crank mechanism. Aerofoil incidence was measured using a potentiometer geared to the model support.

Each model was instrumented with 30 ultraminiature pressure transducers (a mixture of ENTRAN EPI-080-5 and KULITE XCS-093-PSI G), which were installed below the surface at the center span. There were a total of 20 transducers installed on the upper (lee) surface. Each transducer was fitted with a temperature compensation

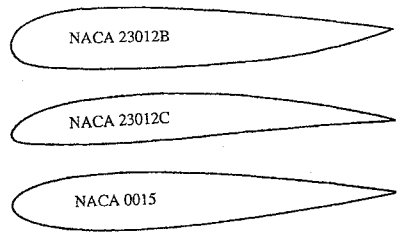

Fig. 4 NACA 23012B, 23012C, and 0015 aerofoil profiles.

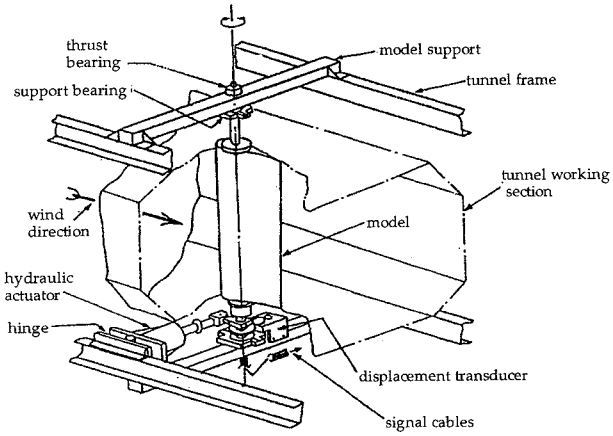

Fig. 5 University of Glasgow Handley–Page wind tunnel and unsteady aerodynamics facility.

module to minimize the changes in zero offset and sensitivity with temperature. Offsets were recorded with the tunnel switched off, and to further eliminate thermal drift, the offsets were regularly re-recorded as a sequence of tests was carried out. After amplification and filtering, the outputs of the pressure transducers were passed to a sample-and-hold module. Data logging was performed using a DEC MINC; 256 samples per transducer per run at up to 550 Hz were recorded. For each test case, data from five runs were taken. After sampling, the data were processed, averaged, and stored on a DEC MicroVAX in a form suitable for analysis.

Smoke Flow Visualization Tests

The smoke flow visualization tunnel was based on a design by Head (reported in Head and Bandyopadhyay[12]) and consisted of a sealed room containing a 1 × 1 m perspex tube with one end open to the atmosphere via a 9:1 c ontraction. A fan was placed a short distance from the downstream end of the tube. Air sucked through the tube by the fan was vented into a small chamber and out into the atmosphere through filters. Smoke was injected into the tunnel from a tube spanning the end of the contraction. The NACA 0015 model under test was placed about 1 m downstream of the end of the contraction and was pitched about the quarter-chord point using a stepper motor linked to a reduction gear box (Green[13]). The chord length of the model was 0.40 m, and the nominal Reynolds number was 2.0×10^4. The blockage of this model is very high; it is stressed that only gross effects are being investigated. However, a comparison of the results from this model with those of a smaller chord length model (described in Green and Galbraith[8]) show the same overall phenomena.

The flow was illuminated using 500-W halogen lamps shining from above and below the model over the midspan position. Flow patterns were videotaped and digitized at a maximum rate of 25 frames per second.

III. Results

The following sections present pressure data from ramp-down tests of the NACA 23012B and 23012C aerofoil sections. Data from the NACA 0015 are also presented where appropriate. The nominal Mach and Reynolds numbers are 0.12 and 1.5×10^6, respectively.

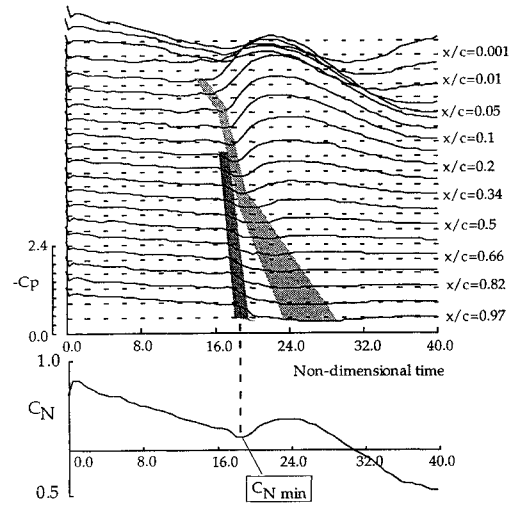

a) $r = -0.009$

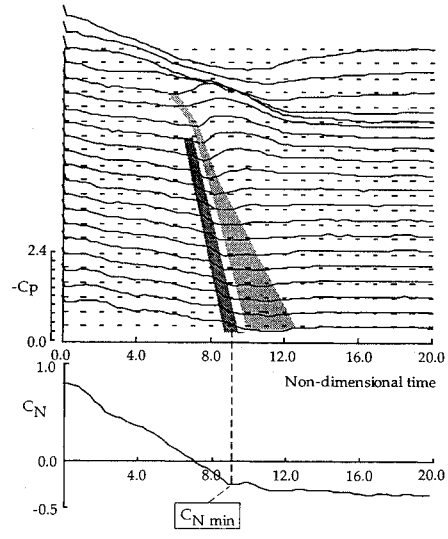

b) $r = -0.03$

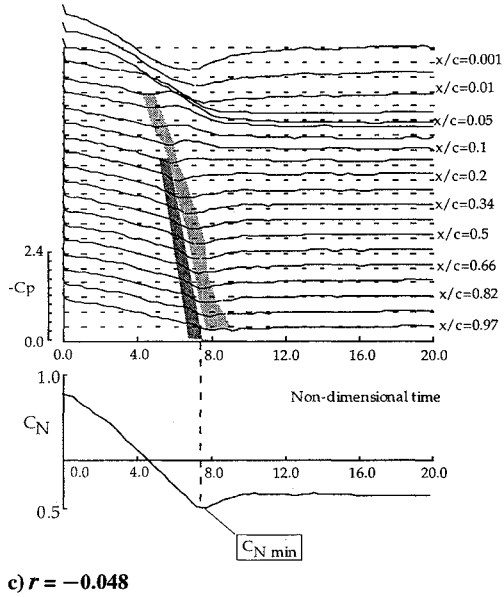

c) $r = -0.048$

Fig. 6 Lee surface pressure transducer traces plotted against nondimensional time during a ramp-down test of the NACA 23012B. Also shown is the normal force coefficient. Reduced pitch rates are $r = -0.009$, -0.03, and -0.048. The attachment and ramp-down waves are indicated. Note how the change in normal force behavior, $C_{N\,min}$, coincides with the passage of the ramp-down wave over the trailing edge: light shading, attachment; dark shading, ramp-down wave.

Occurrence of Minimum Normal Force ($C_{N\,\min}$)

Figures 6a–6c show the individual chordwise pressure transducer traces on the lee surface of the NACA 23012B at $r = -0.009$, -0.03, and -0.048, respectively. Indicated at the bottom of each figure is the normal force coefficient data.

As incidence decreases from 35 deg (i.e., time increases), the individual pressure transducer traces show that suction falls at a nominally constant rate. Shear layer attachment is the most obvious physical phenomenon on the pressure data, and the movement of attachment past a given transducer results in a recovery of suction; the light gray region on each figure highlights the approximate attachment locii. Note that this signal is observed in static tests. Towards the trailing edge the suction recovery is small, and hence attachment is more difficult to locate. It is found that attachment proceeds slowly in the leading-edge region and then moves at a faster rate along the chord from $x/c > 0.1$ (Niven et al.[5] and Green and Galbraith[8]).

It is observed that shortly before attachment there is a period of high rate of decrease of suction. The dark gray zone on Figs. 6a–6c indicates this region. $C_{p\,\mathrm{dev}}$ is defined as the start of the high rate of decrease of suction on each transducer. The maximum rate of decrease of suction within the zone is about five times greater than the nominal value prior to $C_{p\,\mathrm{dev}}$. The first sharp change in $\mathrm{d}(-C_p)/\mathrm{d}t$ characterizing $C_{p\,\mathrm{dev}}$ appears at around $x/c = 0.1$, and it progresses along the chord to the trailing edge. For convenience the zone of high rate of decrease of suction travelling along the chord will be referred to as the ramp-down wave. It is apparent from Figs. 6a and 6b that the rate of movement of the ramp-down wave is significantly faster than that of the attachment signal, although Fig. 6c indicates that attachment moves at about the same rate.

The ramp-down wave is of great importance; Figs. 6a–6c show how the change in the normal force behavior $C_{N\,\min}$ occurs as the ramp-down wave passes over the trailing edge. A more detailed analysis proves to be of interest. Figure 7a shows how $C_{N\,\min}$ correlates with the timing of $C_{p\,\mathrm{dev}}$ and the maximum rate of decrease of suction after $C_{p\,\mathrm{dev}}$ within the ramp-down wave both measured from the trailing-edge transducer. It is clear that $C_{N\,\min}$ occurs in between these two trailing-edge pressure timing points across the entire range of reduced pitch rate. Figures 7b and 7c show the corresponding data for the NACA 23012C and NACA 0015 models. As with the NACA 23012B, $C_{N\,\min}$ shows a strong correlation with the passage of the ramp-down wave over the trailing edge.

Details of the Ramp-Down Wave

As far as the authors are aware, the aforementioned ramp-down wave has not been reported elsewhere. This may well be because little work has been done on either ramp-down motions or unsteady reattachment. It is therefore constructive to present the data as clearly as possible. Note that the data of Schreck et al.[11] also show evidence of the ramp-down wave, although they did not indicate the presence of this feature in their paper.

A popular method of displaying unsteady pressure data is to stack the chordwise pressure distributions to form a pseudo-three-dimensional surface; the pressure manifestations of the aerodynamic phenomena then appear as ridges, peaks, etc. Figure 8 shows the data of Fig. 6b plotted in this way. Incidence decreases (i.e., time increases) from the back to the front of the picture; this perspective is vital if the aerodynamic phenomena are to be seen. Before the formation of the ramp-down wave, the suction along the chord is uniform, and $-C_p$ decreases as incidence decreases. At about 16-deg incidence, leading-edge suction starts to increase sharply, and shortly afterwards the ramp-down wave first appears (indicated on the figure). As time progresses further, the rapid drop in suction caused by the wave results in a local minimum in the chordwise pressure distribution (see later). The end of the ramp-down wave is also indicated. Thus when the data are plotted as shown, the ramp-down wave almost appears as a discontinuity between two different suction levels.

Since the ramp-down wave appears as a change in the rate of decrease of suction, it is more clearly revealed if the pressure data are differentiated with respect to time. Figure 9 shows the data of Fig. 6b in the form of a time/chord contour plot of $\mathrm{d}(-C_p)/\mathrm{d}t$. The leading edge is at the right of the figure, and time increases (i.e., incidence

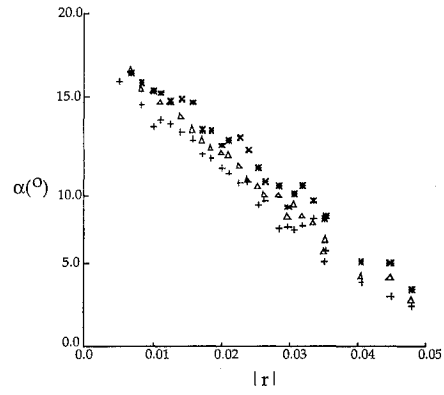

a) NACA 23012B

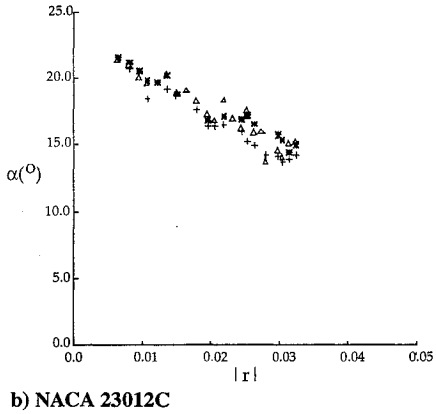

b) NACA 23012C

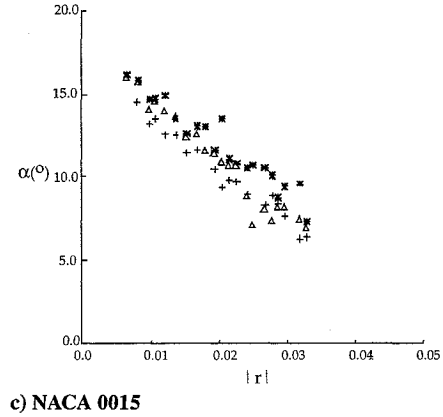

c) NACA 0015

Fig. 7 Correlation of $C_{N\,\min}$ with the rate of change of suction at the trailing edge for the NACA 23012B, 23012C, and 0015. The incidences of the start of the high rate of change of C_p region, the maximum rate of change of C_p, and $C_{N\,\min}$ are shown plotted against reduced pitch rate: Δ, $C_{N\,\min}$; *, $C_{p\,\mathrm{dev}}$ at trailing edge; +, maximum $\mathrm{d}C_p/\mathrm{d}t$ at trailing edge.

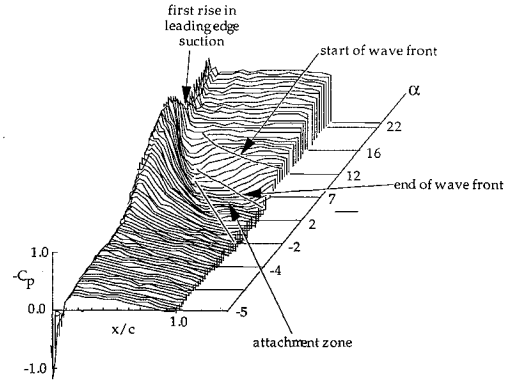

Fig. 8 Chordwise pressure distribution from a $r = -0.03$ ramp-down test of the NACA 23012B plotted as a function of incidence. The rise in leading-edge suction following leading-edge attachment can be clearly seen. The ramp-down wave and attachment waves are indicated.

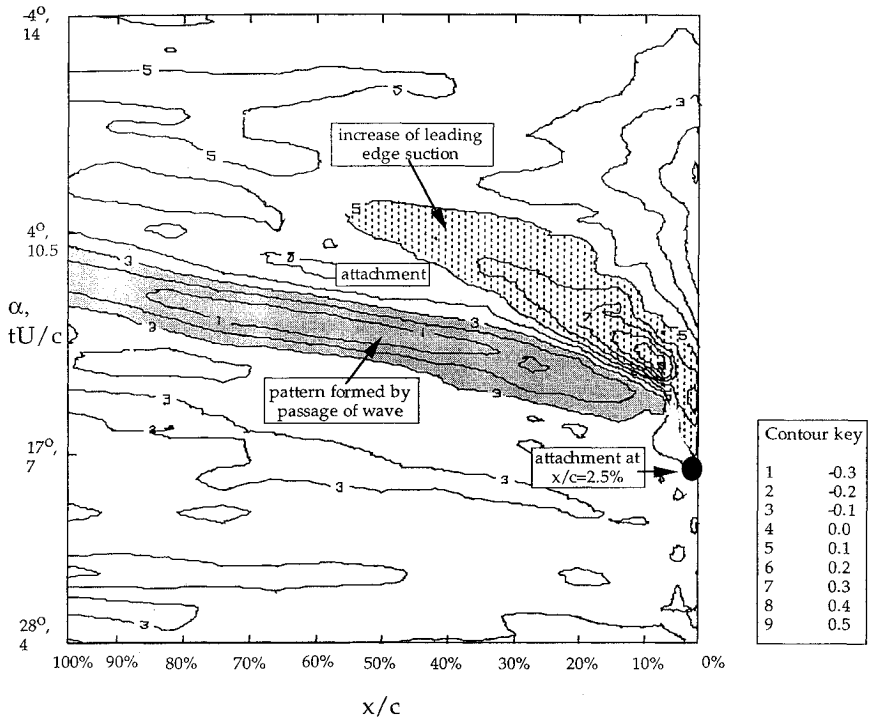

Fig. 9 Time/chordwise position contour plot of rate of change of pressure coefficient. The relevant features are indicated. Ramp-down test of the NACA 23012B at $r = -0.03$.

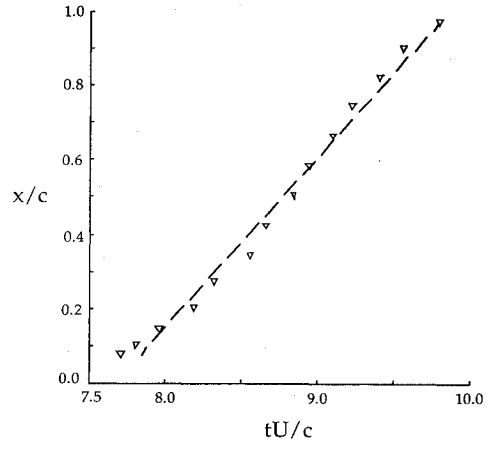

Fig. 10 Locus of ramp-down wave along the chord of the NACA 23012B at $r = -0.03$. The least-squares fit to the data is also shown: gradient = 0.47 and correlation coefficient = 0.98.

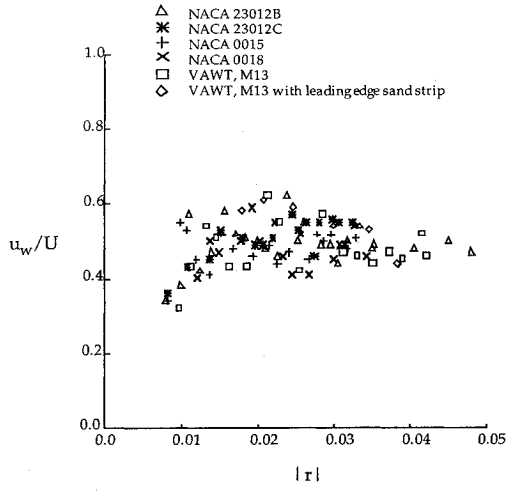

Fig. 11 Ramp-down wave speeds plotted as a function of reduced pitch rate.

decreases) from bottom to top. The first feature indicated is the attachment signal at $x/c = 2.5\%$; the subsequent attachment locus is also shown. The positive contours highlighted after 2.5% chord attachment reflect the increase in suction following flow attachment. The ramp-down wave, indicated by the zone of high negative rate of change of suction, first appears shortly after attachment takes place at $x/c = 2.5\%$. Plotted in this way, the wave is well defined, and it extends from just behind the leading edge to the trailing edge.

The rate of convection of the wave is an important physical value to quantify. To measure the speed of the wave, the timing of some salient feature on the pressure data needed to be measured. Locating the occurrence of $C_{p\,\mathrm{dev}}$ itself was too prone to error, and so the timing of the maximum rate of decrease of suction after $C_{p\,\mathrm{dev}}$ was used. The rate of convection may either be measured directly from a contour plot such as in Fig. 9, or the individual transducer values of the rate of decrease of $-C_p$ may be plotted, and the maximum values pinpointed as the timing marks. The latter method is based on Lorber and Carta's[2] technique for measuring the dynamic stall vortex convection speed and is less subjective than measuring the speed off the contour plot. Figure 10 shows the locus of the maximum values of the individual transducer $\mathrm{d}(-C_p)/\mathrm{d}t$ timing points along the chord, and the least-squares fit to the data. The correlation coefficient is very close to 1, indicating that the rate of movement of the wave along the chord is uniform. The gradient of the fit is the speed of the wave along the chord, and for this particular case it has a value of 0.47. This analysis was repeated across the entire pitch rate range for the NACA 23012B, 23012C, and 0015 aerofoil models. Data were also analyzed for a NACA 0018 profile and the VAWT profile, which has a thickness of 21% and is designed for use on wind turbines. Note that the latter model was also tested with a thick sand strip extending to 2% chord on both surfaces, and these data were also analyzed.

The ramp-down wave speed data for the preceding models are shown in Fig. 11. An obvious feature of the data is the large scatter. It should be noted that differentiation of discrete, sampled data introduces large errors. If the data above $|r| = 0.012$ only are considered, then it may be deduced that the wave speed is independent of the reduced pitch rate over the range considered, and the mean values for the NACA 23012B, 23012C, 0015, 0018, and VAWT

models are 0.49, 0.50, 0.48, 0.47, and 0.46, respectively. In view of the scatter, the differences in these mean values of u_w/U are not significant, and the overall mean value of the ramp-down wave convection speed for all of the models is about half the freestream speed. Note that the average wave speed for the VAWT profile with the leading edge sand strip is 0.52; for the same reasons as stated before, the difference between this value and the clean leading-edge average is insignificant. The data below $|r| = 0.012$ suggest that u_w falls as $|r|$ decreases. It is stressed, however, that at such low values of $|r|$ the ramp-down wave was often poorly defined, and therefore the track of the wave was difficult to measure. Hence the number of data points below $|r| = 0.012$ is quite small, and a dependency of u_w on r at $|r| < 0.012$ can only be suggested.

Flow Visualization

Green and Galbraith[8] presented results of smoke flow visualization tests on a NACA 0015 model at $Re = 1.0 \times 10^4$. These data showed that a significant characteristic of the flow during ramp-down motion was the delayed convection of the bulk of the wake fluid. As a result smoke lines were diverted away from the aerofoil surface. Further testing was carried out to isolate the details of the wake convection during a ramp-down test, and the results are described in this section. A much larger chord model was used, and the nominal test Reynolds number was 2.0×10^4.

Figure 12 shows a sequence of smoke flow pictures from a 40- to 0-deg test at $r = -0.04$. Note that only the first two thirds of the chord are shown. The first frame shows the flow at 20 deg. As incidence decreases, the wake becomes much narrower. At 12-deg incidence, frame (c), an upward deflection of the streamlines is clearly visible. Although the wake boundary streamline becomes turbulent, in the static case it appears almost horizontal. At 4-deg incidence, frame (e), the flow is still fully separated, although the static test at the same incidence [shown in frame (i)] shows a significant amount of attached flow. The ramp-down test at 0 deg shows that

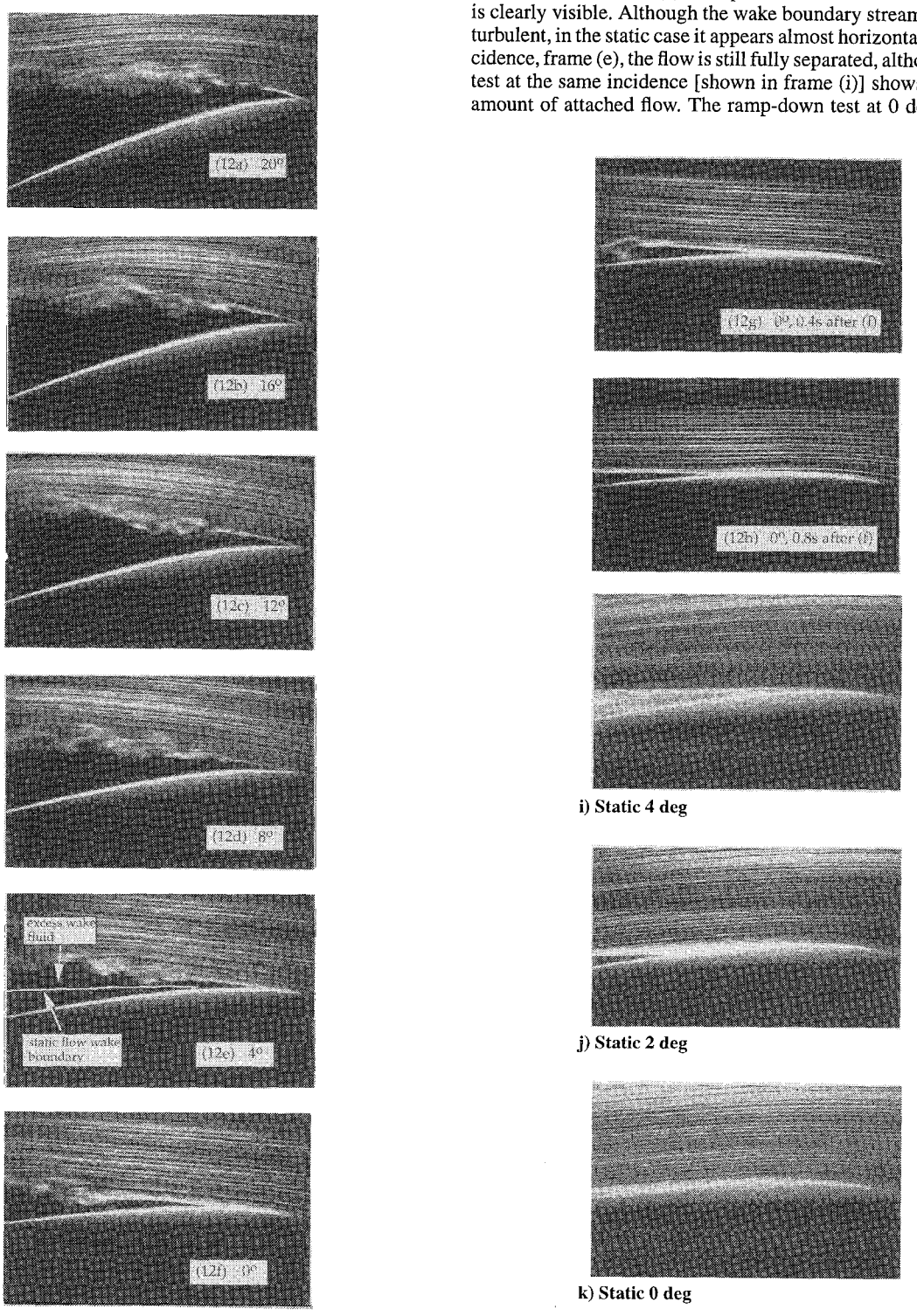

Fig. 12 Sequence of smoke flow visualization pictures of a 40- to 0-deg ramp-down test of a NACA 0015 at $r = -0.04$.

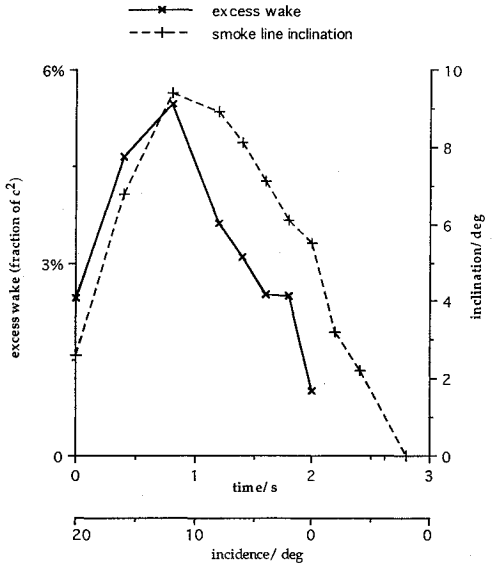

Fig. 13 Excess wake area and streamline inclination above the quarter-chord as a function of time/incidence during a ramp-down test. Test conditions as for Fig. 12.

flow attachment has progressed along the chord towards the trailing edge; the wake is still large, whereas the static test at 0 deg [frame (k)] shows almost no separated flow.

The upward inclination of the smoke lines is caused by the excess fluid within the wake, which in turn is the result of a lack of convection of fluid away from the aerofoil surface. Figure 12e indicates a consistent method of defining the excess fluid within the wake; the excess wake is the area of the wake above the approximate static flow wake boundary. If the amount of this fluid together with the smoke line inclination above a given point are measured, then the wake convection effect may be described. Figure 13 shows the excess wake fluid and streamline inclination above the quarter-chord as a function of time/incidence. Only the data below $\alpha = 20$ deg are shown. As incidence falls, the excess wake fluid increases and reaches a maximum at about 10-deg incidence. The excess wake fluid falls thereafter. The streamline inclination shows a similar trend; above the quarter-chord position, the inclination rises to a maximum at $\alpha = 10$ deg and then falls.

IV. Discussion

The preceding results described a wave observed on pressure data gathered during aerofoil ramp-down motions from the fully separated state to attached flow. As the wave passes over the trailing edge, there is a distinct change in the normal force/incidence behavior, which indicates a transition from bluff body flow behavior to that of a partially separated aerofoil flow. Above $|r| = 0.012$ the speed of the wave was shown to be independent of model type and reduced pitch rate and had a mean value of half the freestream speed.

The flow visualization data (Figs. 12 and 13) show that ineffective convection of wake fluid away from the aerofoil is an important characteristic of dynamic reattachment. If attachment was simply delayed and wake convection was not important, then the distortion of the external streamlines would not be observed. The flow visualization data therefore show two fundamental effects, and dynamic reattachment consists of a wake convection process followed by attachment itself. The Reynolds number difference between the flow visualization data and the pressure data has two important effects: attachment will occur at lower incidence at the lower Reynolds number, and the mechanism of entrainment of wake fluid by the freestream at the higher Reynolds number will be more effective as the shear layer will be turbulent. However, it may be expected that the gross phenomena are the same, and only the quantitative descriptions differ between the pressure data and flow visualization tests.

Figure 9 shows that there is approximately one chord length of aerofoil travel between the first observation of movement of attachment at the leading edge and the first observation of the ramp-down wave. Therefore, a consideration of the conditions at which the preceding wave is first observed is required. At wave onset, the pressure distributions show a significant build up of suction over the leading edge, whereas the suction within the separated flow region is almost uniform. Figure 14 shows the chordwise suction distributions over the NACA 23012B just after the first appearance of the ramp-down wave and 2 deg later. At 14-deg incidence, attachment is at approximately 7% of chord, and at 12 deg it is at about 18% of chord. At 14 deg the ramp-down wave has started to move along the chord, and a minimum appears in the suction distribution. At 12-deg incidence the wave-related suction minimum has deepened and moved further along the chord. The pressure within the wake in a steady flow is largely governed by the fluid velocity at the wake boundary. It is suggested here that the pressure distributions of Fig. 14 indicate a curved wake boundary, the curved boundary being a result of the presence of excess wake fluid; fluid ahead of the enlarged wake partially stagnates and then accelerates over it. This would result in a streamline distortion similar to Fig. 12. As a result there is a pressure gradient along the length of the wake, with higher suction towards the trailing edge; a result of this pressure gradient is that wake fluid is accelerated along the chord towards the trailing edge.

Thus to complement the observations from the flow visualization data, it is suggested that the ramp-down wave is indicative of convection of wake fluid over the aerofoil surface. Figure 15 shows how the flow may appear during a ramp-down test. As the flow attaches over the leading edge, fluid accelerates over the leading edge and then encounters the enlarged wake, resulting in the pressure distributions of Fig. 14. Note that the ramp-down wave convects at a significantly faster rate than attachment; if the ramp-down wave indicates enhanced convection of wake fluid, then a "thin" area of wake fluid may be left behind the ramp-down wave. An important note is that the clarity of the ramp-down wave became very poor at

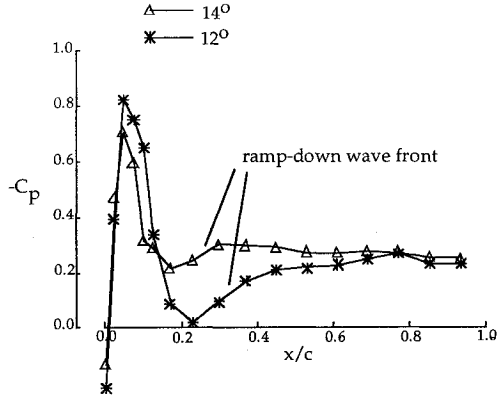

Fig. 14 Lee surface chordwise pressure distributions at 14- and 12-deg incidence during a ramp-down test of the NACA 23012B at $r = -0.03$. The ramp-down wave front is indicated.

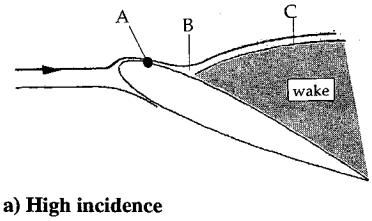

a) High incidence

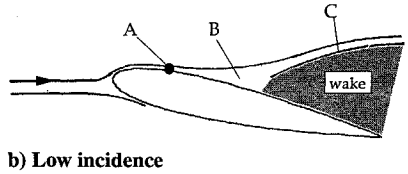

b) Low incidence

Fig. 15 Possible flow patterns during ramp-down motion test; A, attachment position; B, thinned out region of the wake; and C, boundary of the main part of the wake.

low values of $|r|$. As $|r|$ becomes very small, there is a return to static flow behavior, and convection of wake fluid off the aerofoil surface will become a more gradual process. Hence it may be expected that a feature on the pressure data indicating convection of wake fluid would gradually disappear as reduced pitch rate tends to zero.

The pressure data presented by Schreck et al.[11] show similar features to those on the present data, even though their Reynolds number is significantly lower (6.9×10^4 compared with 1.5×10^6). Indeed, their flow conditions more closely represent the flow conditions of the flow visualization data described earlier. Increasing the present flow visualization Reynolds number to 4×10^4 resulted in similar flow patterns to those at $Re = 2 \times 10^4$. This lends weight to the suggestion that the ramp-down wave is caused by convection of wake fluid over the aerofoil surface, although ideally flow visualization and pressure data are needed from the same experiment.

Green and Galbraith[8] showed that the contribution of the windward surface to the overall normal force was significant; suction on the windward surface was observed to rise as incidence decreases. The flow over the windward surface must adjust to the pressure at the trailing edge (which is controlled by the wake), and so when the trailing-edge pressure changes relatively quickly, the flow over the windward surface experiences a rapid change in behavior. The wake may therefore be considered to act as a buffer between the windward surface and the events on the lee surface, so that the windward surface shows no significant change in behavior until the ramp-down wave passes over the trailing edge.

Finally, some details of the reattachment itself will be discussed. Turbulent flow detachment has been described as a gradual change from attached to detached flow (Kline et al.[14]); zero wall shear stress is the result of the averaging to zero of the local unsteady turbulent motions, and hence detachment takes place over a zone, rather than at a point. This applies to reattachment as well, although now the turbulent scales within the separated shear layer cause even greater fluctuations. Thus Niven et al.[5] postulated that reattachment during ramp-down motions consisted of a process in which the turbulent scales were damped from those of a free shear layer to those of an attached boundary layer. It has been observed that attachment moves around the leading-edge region relatively slowly and then accelerates to a constant rate above $x/c = 0.1$. To complement this, the present paper has shown that the first observation of the ramp-down wave precedes the more rapid rate of attachment along the chord. Attachment cannot proceed while wake fluid is still present immediately ahead of the attachment position. Thus the functional variation of attachment rate on reduced pitch rate (initially observed by Niven et al.[5] and Niven and Galbraith[6] and shown in Fig. 2) must be a consequence not only of the change of scales of the turbulence within the shear and boundary layers described earlier but also of the presence and convection of the wake fluid.

V. Conclusions

The flow over an aerofoil during ramp-down motion from the high incidence, fully separated state to the fully attached state is characterized by an extension of the bluff body behavior to low incidence. The condition of negative lift at large positive incidence may be the result. Surface pressure data show a wave, named the ramp-down wave, travelling from the leading-edge region to the trailing edge, and the speed of this wave is independent of reduced pitch rate and model type in the reduced pitch rate range $0.012 < |r| < 0.047$. Smoke flow visualization data show that the wake is significantly larger than in the static case and that the excess wake fluid is gradually washed away from the aerofoil. It is suggested that the ramp-down wave is caused by convection of wake fluid over the aerofoil surface and that the role of attachment in the leading edge is important in speeding up the rate of convection, effectively causing the observed wave.

Acknowledgments

This work was performed with the financial assistance of the Science and Engineering Research Council (Grant GR/H16711). The support of Westland Helicopters, and in particular T. S. Beddoes, is appreciated. The authors would like to take this opportunity to acknowledge the assistance of the technical staff of the Department of Aerospace Engineering, University of Glasgow.

References

[1]McCroskey, W. J., McAlister, K. W., Carr, L. W., Pucci, S. L., Lambert, O., and Indergrand, R. F., "Dynamic Stall on Advanced Airfoil Sections," *Journal of the American Helicopter Society*, Vol. 26, No. 3, 1981, pp. 40–50.

[2]Lorber, P. F., and Carta, F. O., "Unsteady Stall Penetration Experi ments at High Reynolds Number," United States Air Force Office of Scientific Research TR-97-1202, United Technologies Research Center R87-956939-3, East Hartford, CT, April 1987.

[3]Green, R. B., Galbraith, R. A. McD., and Niven, A. J., "Measurements of the Dynamic Stall Vortex Convection Speed," *Aeronautical Journal*, Vol. 96, No. 958, 1992, pp. 319–325.

[4]Galbraith, R. A. McD., Gracey, M. W., and Leitch, E., "Summary of Pressure Data for Thirteen Aerofoils on the University of Glasgow's Aerofoil Database," Univ. of Glasgow, Dept. of Aerospace Engineering, Rept. 9221, Glasgow, Scotland, UK, June 1992.

[5]Niven, A. J., Galbraith, R. A. McD., and Herring, D. G. F., "Analysis of Reattachment During Ramp-Down Tests," *Vertica*, Vol. 13, No. 2, 1989, pp. 187–196.

[6]Niven, A. J., and Galbraith, R. A. McD., "Experiments on the Establishment of Fully Attached Aerofoil Flow from the Fully Stalled Condition During Ramp-Down Motions," *Proceedings of the 17th International Congress of the Aeronautical Sciences* (Stockholm, Sweden), AIAA, Washington, DC, 1990, pp. 653–662.

[7]Green, R. B., and Galbraith, R. A. McD., "A Demonstration of the Effect of Wind Tunnel Constraint on Unsteady Aerodynamics Experiments," *Aeronautical Journal*, Vol. 98, No. 973, 1994, pp. 83–90.

[8]Green, R. B., and Galbraith, R. A. McD., "Phenomena Observed During Aerofoil Ramp-Down Motions from the Fully Separated State," *Aeronautical Journal*, Vol. 98, No. 979, 1994, pp. 349–356.

[9]Ahmed, S., and Chandrasekhara, M. S., "Reattachment Studies of an Oscillating Airfoil Dynamic Stall Flowfield," AIAA Paper 91-3225, Sept. 1991.

[10]Ahmed, S., and Chandrasekhara, M. S., "Reattachment Studies of an Oscillating Airfoil Dynamic Stall Flowfield," *AIAA Journal*, Vol. 32, No. 5, 1994, pp. 1006–1012.

[11]Schreck, S. J., Faller, W. E., and Luttges, M. W., "Dynamic Reattachment on a Downward Pitching Finite Wing," AIAA Paper 94-1907, June 1994.

[12]Head, M. R., and Bandyopadhyay, P., "New Aspects of Turbulent Boundary Layer Structure," *Journal of Fluid Mechanics*, Vol. 107, June 1981, pp. 297–338.

[13]Green, R. B., "A Stepper Motor Based System for Rapid Pitching of Wind Tunnel Models," Univ. of Glasgow, Dept. Aerospace Engineering, Rept. 9402, Glasgow, Scotland, UK, March 1994.

[14]Kline, S. L., Bardina, J., and Strawn, R., "Correlation and Computation of Detachment and Reattachment of Turbulent Boundary Layers on Two-Dimensional Faired Surfaces," AIAA Paper 81-1220, June 1981.